Ground behaviour and settlements analysis on tunnelling of shallow-buried metro in Tashkent city

Mirzakhid Miralimov*, and *Normurodov* Shakhboz

Tashkent State Transport University, Tashkent, Uzbekistan

Abstract. This paper proposed a calculation method that reflects the process of deformations of the soil mass and subsidence of the ground's surface around the shallow subway tunnels and their study, taking into account the engineering and geological conditions of the construction site on the third line of Tashkent metro. The vertical ground displacements of soil mass and zone of destruction (instability) around the hole of the running tunnel of the metro located at different depths were determined. As a result of the numerical calculations performed, the settlements of the ground's surface were determined during tunneling by the shield method. It was found that the maximum value of the trough of the ground's surface decreases with an increase in the depth of the tunnel. This is because with deep tunneling, settlements are largely determined by the decrease in the vertical pressure of the soil on the tunnel due to the formation of a limited disturbed zone around the tunnel hole.

1 Introduction

Today, an ever-expanding Tashkent with an increasing population and cars is facing the problem of traffic jams, which can seriously cause large economic and social losses. To solve this problem, various bridges, overpasses, and new roads are being built, and the city's appearance is changing more and more. Tashkent is getting wider and bigger. The development strategy of the new Uzbekistan for 2022-2026 put forward by the President of our country Shavkat Mirziyoyev is aimed at increasing the effectiveness of progressive reforms, bringing the development of the country and society to a new level. Currently, three metro lines are operating in Tashkent: Chilanzar, Uzbekistan, and Yunusabad. Recently, the Yunusabad line from the Shahristan station to the Turkiston station was extended, the Uzbekistan line at the Dustlik station docked with a section of the circle line, and the Chilanzar line joined the Sergeli branch. The first stage of the circle line and the extended section of the Chilanzar line to the Sergeli residential area is located on the Holocene flat terrace on the overpasses. The remaining promising areas are located in the thickness of the 20 m Tashkent terrace in a reliable layer of loess (Fig.1).

Considering the difficult engineering-geological and hydro-geological conditions of construction on the section of the Yunusabad metro line from the Shahristan station to the

*Corresponding author: mirzakhid_miralimov@yahoo.com

Turkiston station, the tunnels of the closed work method were built using a tunnel-boring mechanized complex (TBMC) with a face load [1]. For tunneling, a Herrenknecht mechanized shield with a soil load is used. The drilling diameter in the penetration is 5.9 m, and the distance between parallel single-track tunnels is 12.9 m. The average depth of the tunnel from the ground to the tunnel contour is 15 m.

Prediction and evaluation of possible impacts on surface structures during tunneling, especially shallow tunnels, is an important issue in the design, construction, and operation of shallow tunnels. The change in the stress-strain state (SSS) of the soil massif surrounding the tunnel hole under construction and the formation of the displacement field associated with it have a very significant effect on the massif, the manifestation of which can reach the earth's surface with the formation of t ground-settlement trough. It is obvious that the magnitude of displacements on the earth's surface will be determined by the level of deformation disturbances in the soil massif directly adjacent to the tunnel. Having found them, we can estimate the magnitude of displacements on the earth's surface and soil massif surrounding the tunnel hole under construction.

Among the large variety of numerical methods that have found their application in geomechanics, perhaps only three of them should be highlighted - this is the finite difference method, method of boundary integrals, and finite element method. The finite difference method, which is used, as a rule, in rigid-plastic problems, allows one to approximately solve differential equilibrium equations by switching to equations in finite differences after constructing meshes of lines, at the intersection of which stress components are determined. The most popular numerical method in geomechanical problems is the finite element method [1-3]. The wide application in the practice of calculations of soil masses confirms its relevance in the problems considered in this work.

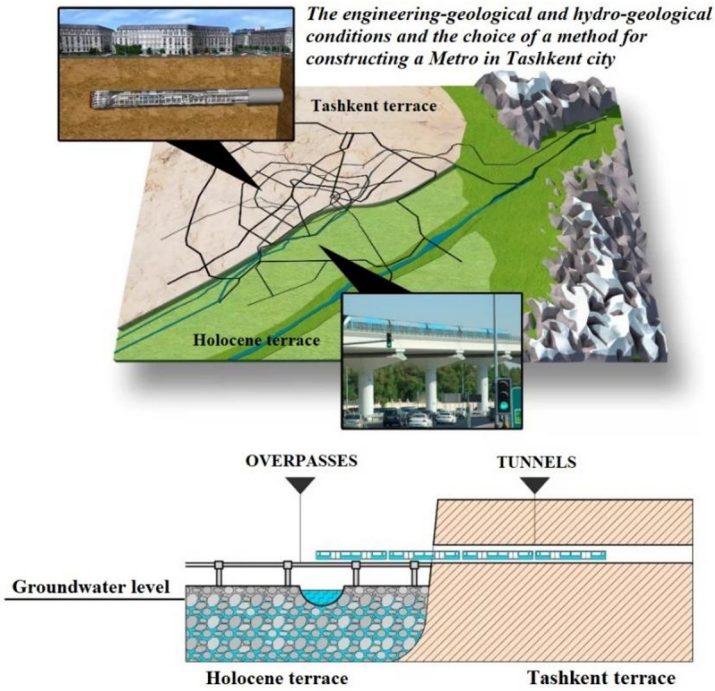

Fig. 1. Underground and elevated lines of the Tashkent metro

2 Objects and methods of research

At the same time, the stress-strain state of untouched soil massif under the action of initial stresses without a hole is first determined, then an excavating is carried out in it, and an additional stress in soil massif are determined from the "removed" stresses on its contour. The sum of the initial and additional stresses solves the problem [4-7]. The desired components of the total stresses in the soil area *S* (Fig. 2) can be represented, as indicated above, as the sum of two terms:

$$\sigma_y = \sigma_y^{(0)} + \sigma_y^{(1)} \qquad \sigma_x = \sigma_x^{(0)} + \sigma_x^{(1)} \qquad \tau_{xy} = \tau_{xy}^{(0)} + \tau_{xy}^{(1)} \tag{1}$$

where $\sigma_x^{(0)}, \sigma_y^{(0)}, \tau_{xy}^{(0)}$ are the initial stresses that acted in the undisturbed mass before the formation of the tunnel hole; $\sigma_x^{(1)}, \sigma_y^{(1)}, \tau_{xy}^{(1)}$ are the additional (removable) stresses caused by the formation of a hole.

Based on the foregoing, the calculation scheme of a tunnel hole is, in the general case, a plane simulating the massif weakened by a hole. The removed stresses are applied to the line of boundary C_L, and external forces can also be applied to the boundary C_P, if necessary.

In soil massif with an average specific gravity γ, the vertical and horizontal components of the body forces from earth pressure at a certain depth can be determined by the well-known formulas:

$$\sigma_y^{(0)} = \gamma H;\ \sigma_x^{(0)} = \lambda \gamma H \tag{2}$$

where H is depth in consideration point of massif; γ is average specific gravity of the massif; λ is lateral pressure coefficient.

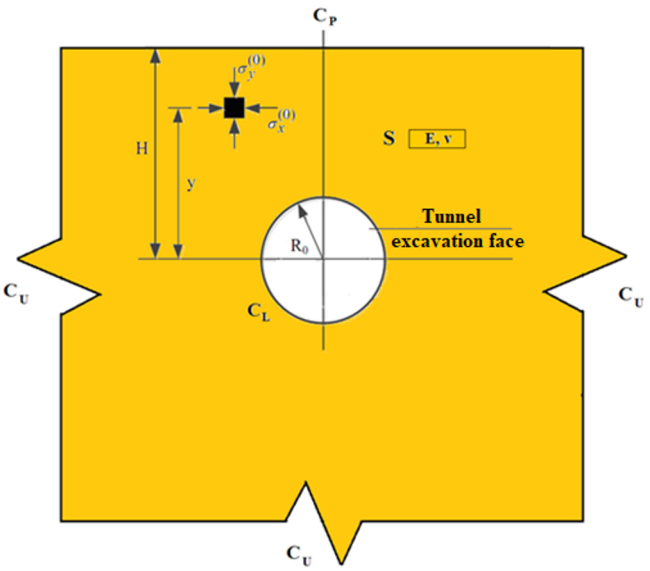

Fig. 2. The scheme for determining the stress-strain state around excavated tunnel hole

The loads applied to the considered part of massif can be specified both by the boundary normal and tangential forces and by the distributed forces from the weight of soil. On the remote lateral boundaries *Cu* of considered area *S*, the corresponding conditions are modeled that prohibit displacements along normal to these boundaries. If the mass is layered, then the stresses change significantly from layer to layer, and the more, the more their elastic characteristics differ. Therefore, when the hole for the tunnel intersects soil layers with different initial stress state, the stress distribution around the hole contour differs significantly from the homogeneous model. The elastic linear model is based on Hooke's law of isotropic linear elasticity.

The model includes two constant stiffness parameters: deformation modulus *E* and Poisson's ratio υ [8]. Analysis of the stress state by the finite element method satisfies the conditions of the static equilibrium condition. It makes it possible to evaluate stress changes caused by varying elastic properties, inhomogeneity, and geometric shapes. Thus, by specifying the forces at each node from the self-weight of soil and at the area's boundaries, a system of joint equations based on a common stiffness matrix can be solved regarding displacements of each node.

If the calculation results are considered in a different form, then the relationship between the stresses in Cartesian and polar coordinate systems (Fig. 3, b) is obtained from the transformation formulas:

$$\left.\begin{matrix}\sigma_r \\ \sigma_\theta\end{matrix}\right\} = \frac{\sigma_1+\sigma_2}{2} \pm \frac{\sigma_1-\sigma_2}{2} cos2\theta$$

$$\tau_{r\theta} = -\frac{\sigma_1-\sigma_2}{2} sin2\theta \qquad (3)$$

Once the displacements are found, each element's stresses can be determined. The mesh of soil area is carried out by isoparametric finite elements (Fig.3, a) [9, 10]. The well-known Mohr-Coulomb model can be considered a first-order approximation concerning the real behavior of the soil [8, 11]. The well-known Mohr-Coulomb model can be considered a first-order approximation concerning the real behavior of the soil [12]. This elastoplastic model requires knowledge of four main input parameters, namely, the deformation modulus E, Poisson's ratio *υ*, cohesion *C*, and the angle of internal friction *φ*.

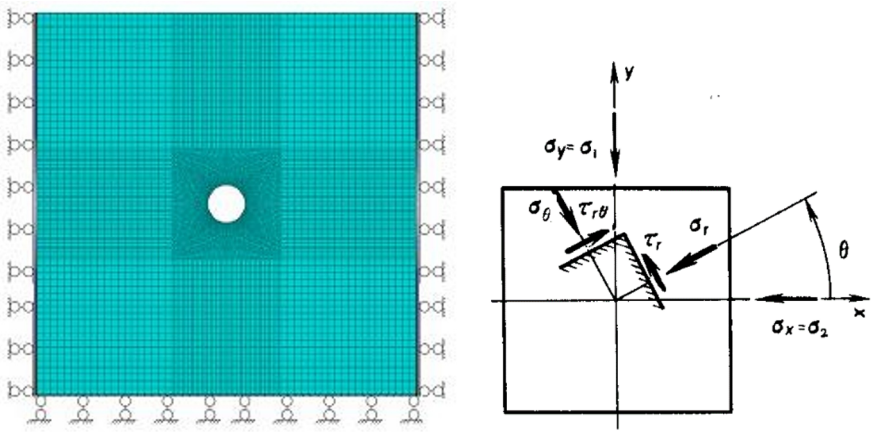

a) *b)*

Fig. 3. Finite element area (a) and stress representation scheme in Cartesian and polar coordinate systems (b)

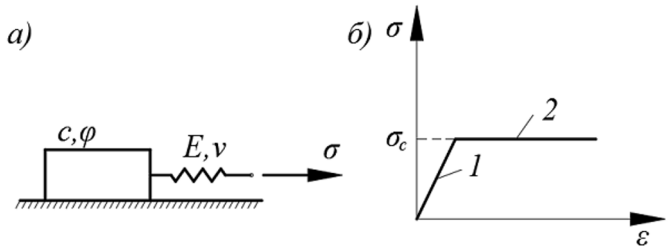

1 is area of elastic deformations; 2 is area of plastic deformations

Fig. 4. Structural scheme (a) and stresses diagram of elasto-plastic model (b)

In the general case, when opening a hole in a soil mass, two zones are distinguished (Fig. 4): elastic - stable 1 and plastic - unstable 2, in which the stress distribution obeys the Hooke's law ($\sigma = E\varepsilon$) and the law of strength - Mohr-Coulomb condition ($\tau_{\text{пр}} = \sigma_n tg\varphi + C$) [13]. Here on the shear areas: τ_{lm} is the limiting shear stress, σ_n is the normal stress.

If the strength of the soil material is determined only by the maximum and minimum principal stresses, then the Mohr-Coulomb condition can be written in the following form:

$$\sigma_1 - \sigma_2 = (\sigma_1 + \sigma_2 + 2\sigma_c)\sin\varphi \qquad (4)$$

In this case, the principal stresses, as is known, are expressed in terms of the stress components along two mutually perpendicular areas by the dependencies:

$$\left.\begin{matrix}\sigma_1\\ \sigma_2\end{matrix}\right\} = \frac{1}{2}(\sigma_x + \sigma_y) \pm \frac{1}{2}\sqrt{(\sigma_x - \sigma_y)^2 + 4\tau^2_{xy}} \qquad (5)$$

Stresses are calculated at the center of each finite element. With known stresses field within the study area and given limit state conditions, it is possible to estimate the soil's strength at each massif point [14]. Assuming, for example, that the destruction of rocks occurs due to shear, knowing the limiting values of shear resistance for the soil of different sections of the massif, and determining the effective shear stresses for most dangerous areas in the elements of mesh, we can find the values of safety factors for these points:

$$\eta = \frac{\tau_{lm}}{\tau} \qquad (6)$$

In the simplest case, these data make constructing lines of equal soil safety factors possible at points. Areas with η>l indicate that the soil has a margin of safety; at η=l, the limit state occurs at points, and the areas with η<l are unstable.

3 Results and discussion

Let's consider the problem of determining the stability of tunnel excavation, which was carried out using the Herrenknecht (TBMC). In the course of solving the problem, the initial stresses field, zones of limiting states in the vicinity of the tunnel hole, and vertical displacements of the surface of soil mass were calculated. In this case, the main linear dimensions of the model are accepted as follows: width of the model (dimension in the direction of the X-axis) - 100 m; model height (dimension in the direction of the Y-axis) - 70 m. For this, the physical and mechanical properties of soil on the tunnel route between Turkistan and Yunusabad stations were used, which are presented in [15, 16]. The depth of

the tunnel varies from 8 to 22 m. Figure 5 shows numerical finite element models of massif with tunnels at various depths.

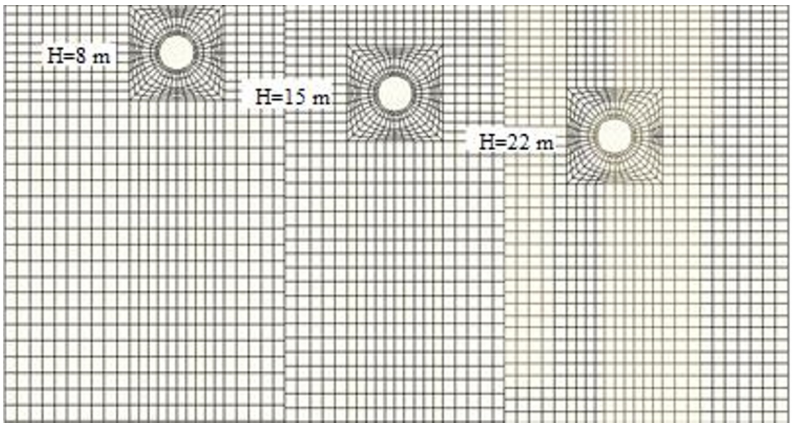

Fig. 5. Numerical models of soil massif with tunnel hole on various depths

Further, due to calculations, local zones of destruction around the tunnel were found. These zones are expressed through certain values of soil safety factors η, which are formed due to plastic failure according to the Mohr-Coulomb strength (limiting state) condition (Fig. 6).

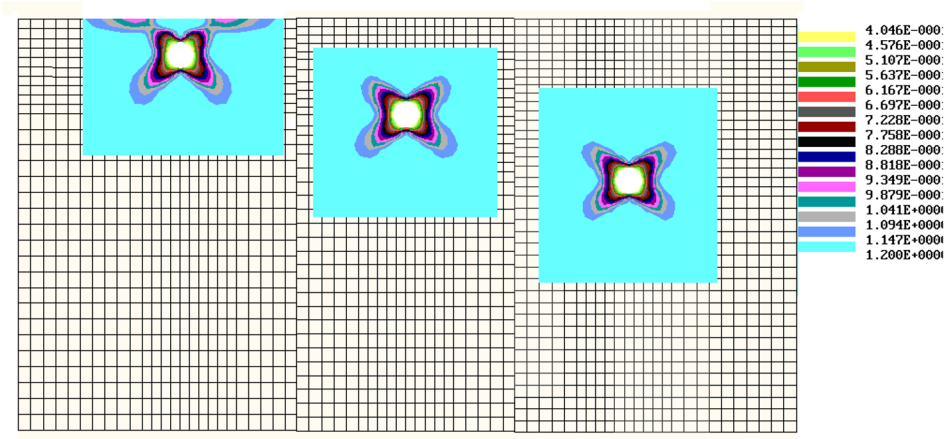

a) H=8 m *b) H=15 m* *c) H=22 m*

Fig. 6. Izochromes of safety factors η for the given area at tunneling depths

The accounting for plastic conditions with changes in soil deformation parameters for each case ($H = 8\,m, 15\,m, 22\,m$) shows that they significantly changed the stress-strain state of soil around the tunnel. The zone of instability around the tunnel hole becomes limited as the depth increases.

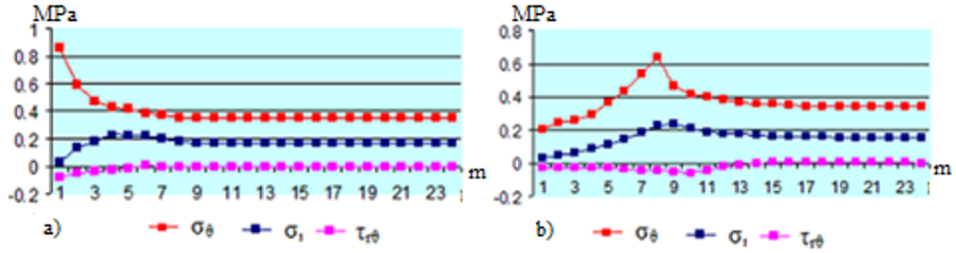

Fig. 7. Distribution of tangential, radial, and rotational stresses around the tunnel hole (θ=0°, H=8 m) at deformation zones: a) elastic, b) plastic

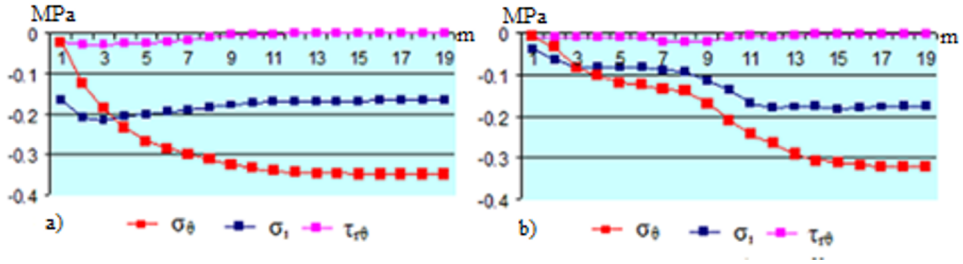

Fig. 8. Distribution of tangential, radial, and rotational stresses around the tunnel hole (θ=180°, H=8 m) at deformation zones: a) elastic, b) plastic

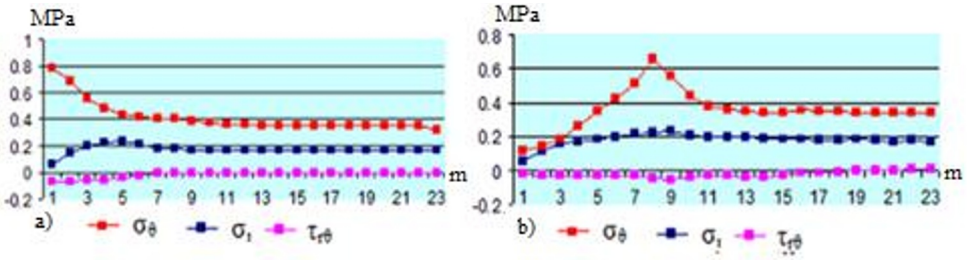

Fig. 9. Distribution of tangential, radial, and rotational stresses around the tunnel hole (θ=0°, H=15 m) at deformation zones: a) elastic, b) plastic

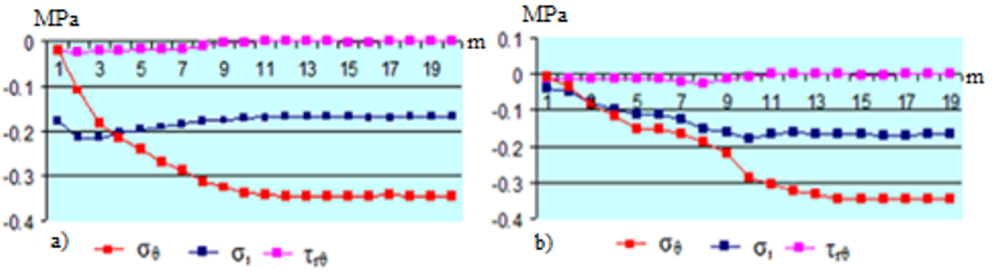

Fig. 10. Distribution of tangential, radial, and rotational stresses around the tunnel hole (θ=180°, H=15 m) at deformation zones: a) elastic, b) plastic

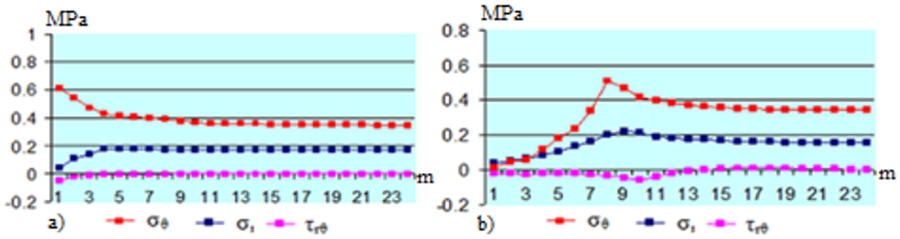

Fig. 11. Distribution of tangential, radial, and rotational stresses around the tunnel hole (θ=0°, H=22 m) at deformation zones: a) elastic, b) plastic

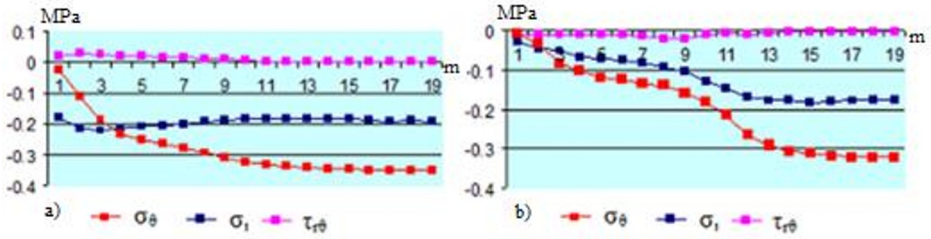

Fig. 12. Distribution of tangential, radial, and rotational stresses around the tunnel hole (θ=180°, H=22 m) at deformation zones: a) elastic, b) plastic

Fig. 7-12 shown in the form of diagrams the distribution of values of radial, tangential, and shear stresses when the tasks were solved without taking into account local damage in the soil area around the tunnel. The analysis of diagrams shows that the formation of plastic deformation area leads to a decrease in the stress level near the hole contour compared to the solution of an elastic problem. The maximum stresses move deep into the mass to the interface between elastic and plastic areas. Also, it was found that the maximum value of the trough of the ground's surface decreases with an increase in the depth of the tunnel (Fig. 13).

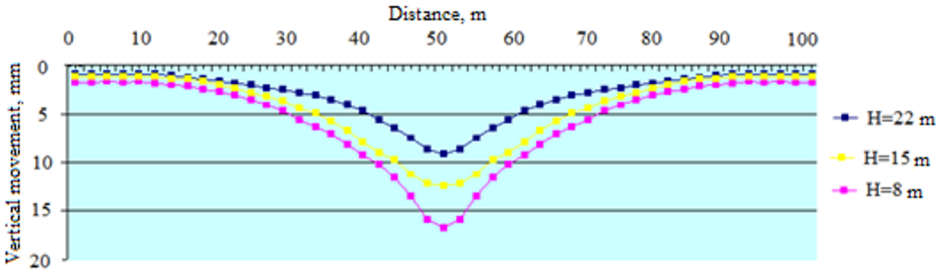

Fig. 13. Troughs of vertical deformation of earth's surface at different tunnel depth: $H = 8\ m, H = 15\ m, H = 22\ m$.

4 Conclusion

The computational model has been developed to study ground behavior and stress-strain state in zones of tunnel holes located at soil massif and conducted settlements analysis on tunneling of shallow-buried Metro in Tashkent city. As a result of the numerical calculations performed, the settlements of the ground's surface were determined during tunneling by the shield method. It was found that the maximum value of the trough of the

ground's surface decreases with an increase in the depth of the tunnel. This is because with deep tunneling, settlements are largely determined by the decrease in the vertical pressure of the soil on the tunnel due to the formation of a limited disturbed zone around the tunnel hole.

References

1. Altaee A., Fellenius B. H., and Salem H. Finite element modeling of lateral pipeline-soil interaction. In proceedings of the international conference on offshore mechanics and arctic engineering, pp. 333-342, (1996).
2. Li J. C., Li H. B., Ma G. W., and Zhou Y. X. Assessment of underground tunnel stability to adjacent tunnel explosion. Tunn Undergr Sp Tech Vol. 35, pp.227–234. (2013).
3. Miralimov M. Strength calculation method of reinforced concrete structures of Tashkent underground tunnels with different stages of stress condition. In IOP Conference Series: Materials Science and Engineering, Vol. 615(1), p. 012083, (2019)
4. Kolymbas D. Tunnelling and tunnel mechanics: A rational approach to tunnelling. Springer Science and Business Media. (2005).
5. Fotieva N. N., and Sheinin V. I. Distribution of stresses in the lining of a circular tunnel when driving a parallel tunnel. Soil Mechanics and Foundation Engineering, Vol. 3(6), 417-422. (1966).
6. Verruijt A., and Booker J. R. Surface settlements due to deformation of a tunnel in an elastic half plane. Geotechnique, Vol. 48(5), pp.709-713. (1998).
7. Pestryakova E. A, Kharitonov S. S., Titov E. Y. Methods for estimating sediment during tunneling using a mechanized tunneling. Russian journal of transport engineering. Vol. 6(3), pp.1-12 (2019).
8. Bulychev N.S. Mechanics of underground structures: Studies for universities. – 2nd ed., reprint. and additional – M.: Nedra. p. 382, (1994).
9. Barkanov E. Introduction to the finite element method. Institute of Materials and Structures Faculty of Civil Engineering Riga Technical University, pp.1-70, (2001).
10. Carroll W. F. A primer for finite elements in elastic structures. John Wiley and Sons. (1998).
11. Miralimov M., Normurodov S., Akhmadjonov M., and Karshiboev A. Numerical approach for structural analysis of Metro tunnel station. In E3S Web of Conferences, Vol. 264, p. 02054, (2021).
12. Guglielmetti V., Grasso P., Mahtab A., and Xu S. (Eds.). Mechanized tunnelling in urban areas: design methodology and construction control. Taylor and Francis. (2008).
13. Broere W. Influence of excess pore pressures on the stability of the tunnel face. In (Re) Claiming the underground space, pp. 759-765, Routledge (2003).
14. Ritter, S. Experiments in tunnel-soil-structure interaction. Doctoral dissertation, University of Cambridge, (2018).
15. Construction of the second stage of the Yunusabad metro line on the section from Shakhristan station to Turkiston station. Section 8. Project of works. Tashkent Metroproekt LLC, p. 120, (2017)
16. Adilov F. F., Miralimov M. H., and Abirov R. A. To the stability of the roadbed reinforced with gabions. In IOP Conference Series: Materials Science and Engineering, Vol. 913(4), p. 042066, (2020).